ELSEVIER Journal of Hazardous Materials A 66 (1999) 227–237

Journal of Hazardous Materials

TWODEE: the Health and Safety Laboratory's shallow layer model for heavy gas dispersion Part 2: Outline and validation of the computational scheme

R.K.S. Hankin [a,*], R.E. Britter [b,1]

[a] *Health and Safety Laboratory, Harpur Hill, Buxton, Derbyshire SK17 9JN, UK*
[b] *Cambridge University Engineering Department, Trumpington Street, Cambridge CB2 1PQ, UK*

Received 23 October 1998; received in revised form 30 October 1998; accepted 4 December 1998

Abstract

Part 1 of this three part paper described the mathematical and physical basis of TWODEE, the Health and Safety Laboratory's shallow layer model for heavy gas dispersion. In this part, the numerical solution method used to simulate the TWODEE mathematical model is developed. The boundary conditions for the leading edge, discussed in part 1, make demanding requirements on the computational scheme used. The flux correction scheme of Zalesak [S.T. Zalesak, Fully multidimensional flux-corrected transport algorithms for fluids, Journal of Computational Physics, 31 (1979) 335–362] is used in TWODEE as this has all the required properties. The TWODEE code is then tested against a number of theoretical and computational benchmark problems.

Keywords: TWODEE; Heavy gas; Shallow layer

1. Introduction

The TWODEE model introduced in part 1 of this paper requires computational solution for industrially useful predictions. Because the boundary conditions specified in part 1 can result in a large depth gradient at the leading edge, care must be taken in choosing a

* Corresponding author.
[1] Supported by the European Union MTH programme (FLADIS).

0304-3894/99/$ - see front matter
PII: S0304-3894(98)00275-1

numerical scheme that eliminates numerical overshoot (which could produce the unrealistic result of negative fluid depths).

2. Numerical solution of equations in conservation form

For simplicity, the one-dimensional system of equations

$$\frac{\partial \boldsymbol{w}}{\partial t} + \frac{\partial \boldsymbol{f}}{\partial x} = 0 \tag{1}$$

is considered, where $\boldsymbol{w}$ and $\boldsymbol{f}$ are vector functions of position and time. If, for example, the following choice is made:

$$\boldsymbol{w} = \begin{pmatrix} h \\ h(\rho - \rho_a) \\ h\rho u \end{pmatrix} \quad \boldsymbol{f} = \begin{pmatrix} hu \\ h(\rho - \rho_a)u \\ h\rho u^2 + \frac{1}{2}g(\rho - \rho_a)h^2 \end{pmatrix} \tag{2}$$

then this is the shallow water equations in one dimension. Other choices for $\boldsymbol{w}$ and $\boldsymbol{f}$ give systems such as the Euler equations.

Numerical solution of this system of equations is not simple and many numerical schemes have been devised; review articles are given by Chock [2] and Woodward and Colella [3]. However, only one scheme will be considered here: that of Zalesak [1].

Finite difference solution schemes for Eq. (1) must make some type of approximation to $\boldsymbol{w} = \boldsymbol{w}(x,t)$, which is a function of both space and time. This is done by discretizing space and time and considering only $\boldsymbol{w}(x_i,t_n)$, where x_i is the ith grid point and t_n the nth timestep. It is standard practice to write $\boldsymbol{w}(x_i,t_n) = \boldsymbol{w}_i^n$. Note that, for fixed i and n, $\boldsymbol{w}_i^n$ is a vector.

2.1. The flux correction scheme of Zalesak

In a frequently cited paper, Zalesak [1] presented an advection scheme that combined the low numerical diffusion of high order schemes with the absence of numerical oscillations typical of low order schemes. This advection scheme was based on the earlier work of Boris and Book [4,5] and Boris et al. [6] but improved upon those works by extending their ideas to multiple spatial dimensions. Many workers in the field of computational fluid dynamics have used his ideas [3,7]. The following paragraph paraphrases Zalesak.

Flux corrected transport [FCT] is a technique that embodies the advantages of both low- and high-order schemes. Fundamentally, FCT calculates the fluxes between adjacent fluid elements by taking a weighted average of a flux as computed by a low order scheme and the flux as computed by a high order scheme. The weighting is done in such a manner as to use the high order scheme unless to do so would result in the creation of overshoots (that is, new extrema in $\boldsymbol{w}$) not predicted by the low order

scheme. The assumption is therefore that any new extrema predicted by the low order scheme are genuine.

The method given by Zalesak by which extrema were avoided was to limit each element of $\boldsymbol{w}$ above and below by $\boldsymbol{w}_i^{\max}$ and $\boldsymbol{w}_i^{\min}$. Briefly, $\boldsymbol{w}_i^{\max}$ is the maximum value that $\boldsymbol{w}_i$ may assume without causing an unacceptable (numerical) overshoot; $\boldsymbol{w}_i^{\min}$ is likewise the minimum allowable value of $\boldsymbol{w}_i$. Here, $\boldsymbol{w}_i$ is a vector and the above characterizations of $\boldsymbol{w}_i^{\max}$ and $\boldsymbol{w}_i^{\min}$ apply for each value of the index i; so, for example, $(\boldsymbol{w}_i)_1 = h_i$ is the depth of the current at grid point i and $(\boldsymbol{w}_i)_2 = h(\rho - \rho_a)$ is the buoyancy per unit area divided by the gravitational field strength. Each component of $\boldsymbol{w}_i$ is thus constrained by the corresponding element of the vectors $\boldsymbol{w}_i^{\max}$ and $\boldsymbol{w}_i^{\min}$. A complete description of the method is given by Hankin [8].

2.2. The two-dimensional shallow water equations in conservation form

For convenience the two-dimensional, non-entraining shallow water equations are restated here. For simplicity, only the case of level ground is considered, viscous forces are neglected, and ground drag assumed to be negligible. All dimensionless constants identified by Hankin [8] are taken to be unity. Defining

$$\boldsymbol{w} = \begin{pmatrix} h \\ h(\Delta\rho) \\ h\rho u \\ h\rho v \end{pmatrix}, \boldsymbol{f} = \begin{pmatrix} hu \\ h(\Delta\rho)u \\ h\rho u^2 + \frac{1}{2}g(\Delta\rho)h^2 \\ h\rho uv \end{pmatrix} \text{ and } \boldsymbol{g} = \begin{pmatrix} hv \\ h(\Delta\rho)v \\ h\rho uv \\ h\rho v^2 + \frac{1}{2}g(\Delta\rho)h^2 \end{pmatrix} \tag{3}$$

where $\Delta\rho = \rho - \rho_a$ is the density difference between the dense layer and that of the ambient fluid, gives

$$\frac{\partial \boldsymbol{w}}{\partial t} + \frac{\partial \boldsymbol{f}}{\partial x} + \frac{\partial \boldsymbol{g}}{\partial y} = 0 \tag{4}$$

for the two-dimensional shallow water equations in conservation form.

These equations are well suited to solution using Zalesak's method. At least one other study, by Webber [9], has used this method for the shallow water equations in one dimension.

2.3. Varying ground elevation and flux correction

Numerical solution of the shallow water equations must account for varying ground elevations—considerations not part of a compressible gas flow calculation. The introduction of ground elevation requires generalizations to be made to Zalesak's original scheme. In essence, allowance must be made for the fact that two quantities—h and $\Delta\rho$—are being advected. This can cause problems when fluid moves over a change in ground elevation that (say) halves the fluid depth across one computational element. Under these circumstances, it is clear that limiting $(\boldsymbol{w}_i)_2 = h\Delta\rho$ is not appropriate; in

essence, Zalesak's limiting process is applied to $(w_i)_2/(w_1)_1 = \Delta\rho$. A full discussion is given by Hankin [8].

3. Validation of the computational scheme

It is now shown that the computational scheme described above accurately simulates the physical model developed in part 1 of this paper. Only the idealized case of zero entrainment will be considered, as several analytical results exist for this case against which the results of the code may be compared. The effects of top- and edge-entrainment may be accounted for separately.

The validation exercises will follow a logical order, first testing the most basic feature of the computational model (the advection scheme). Next, the gravitational forcing terms will be tested by verifying that the momentum and energy of a dense layer behave as expected.

Finally, the code is tested against a number of exact, analytical solutions, as recommended by Roache [10].

The computational scheme described is capable of simulating two-dimensional shallow water flow with a specified densimetric front Froude number. This capability allows the simulation of heavy gas dispersion in two dimensions by a shallow water model.

4. The advection equation

The code under development incorporates several novel features (mostly generalizations and extensions of the flux correction scheme of Zalesak [1] which are detailed by Hankin [8]), and several checks on this new scheme will be presented.

4.1. The advection equation with one scalar quantity

The advection equation governs the transport of a conserved scalar quantity (cloud height in this case) when the velocity field is specified. The velocity field transports the scalar quantity from place to place. Any numerical scheme must solve the advection equation accurately as this underpins the more general case.

If h is the fluid depth at any point and $\boldsymbol{u} = (u,v)$ is the fluid velocity, then the advection equation for h is

$$\frac{\partial h}{\partial t} + \frac{\partial hu}{\partial x} + \frac{\partial hv}{\partial y} = 0, \tag{5}$$

which is the mathematical statement of conservation of fluid volume, written in conservation form. Many review articles [2,3,7,11] discuss different numerical solution schemes for Eq. (5) together with the problems they encounter.

The advection equations—as they stand—admit negative fluid depths but physical considerations show that this is unrealistic. In the same way, the advection scheme does

not explicitly forbid negative depths as artificial extrema are suppressed. This is important: slight numerical oscillations near the leading edge could cause negative fluid depths which can lead to severe numerical problems. [2]

The present approach thus does not require an artificially imposed minimum fluid depth of zero; rather, negative fluid depths are implicitly forbidden by the nature of the problem. This is a desirable feature of any advection solver, both on the grounds of computational efficiency and physical accuracy.

4.2. Tests of computational solutions of the advection equation

In 1983, Chock and Dunker [12] presented a comparison of several methods of solving the two-dimensional advection equation. These workers used a standard test for advection schemes, following Sod [7] and this test was carried out on TWODEE and the results presented by Hankin [8].

The advection scheme recommended by Chock and Dunker was a 'Chapeau function' method (Pepper et al. [13] outline this scheme) and the second choice was that of Zalesak [1]. However, Chock and Dunker warned that "... a severe problem with [the Chapeau function method] is the presence of ripples with negative concentrations." This warning renders that particular method of no use for the present problem.

It is concluded that the best method available for the problem under investigation is the multidimensional flux correction scheme of Zalesak, which is the scheme used here. The performance of Zalesak's scheme as implemented in TWODEE [8] was indistinguishable from that of Zalesak's scheme as implemented by Chock and Dunker.

5. Energy conservation

The present formulation of the shallow water equations includes no statement of conservation of energy: rather, energy conservation arises as a consequence of the four shallow water equations used, if only continuous solutions are considered. It is important to show that energy is conserved in the simulations for much the same reasons as those given above for momentum.

Continuous solutions of the shallow water equations conserve energy:

$$\frac{\partial E}{\partial t} + \nabla\cdot(\boldsymbol{u}E) + \nabla\cdot(\boldsymbol{u}P) = 0, \tag{6}$$

where $K = \frac{1}{2}\rho h u^2$ is the kinetic energy per unit area, $P = \frac{1}{2}(\rho - \rho_a)gh^2$ is the potential energy per unit area and $E = P + K$ is the total mechanical energy per unit area. This equation is proved, and generalized to the entraining case, by Hankin [1].

[2] The shallow water equations are closely related to the Euler equations: the depth of fluid in a shallow water simulation is analogous to the density of fluid in a compressible flow and a hydraulic jump is analogous to a shock front. The phenomenon of depth (density) oscillations near a hydraulic jump (shock front) is not as critical in a compressible flow simulation as a slight amount of numerical oscillation near a shock front will not result in negative densities, because the fluid on the upstream side of a shock has a positive density and can thus 'tolerate' a small amount of oscillation without assuming a negative density anywhere. In contrast, because the fluid depth is zero in front of a leading edge, even very small numerical oscillations may result in negative fluid depths which would stop the simulation.

The fluxes between adjacent fluid elements in flows of industrial interest (such as the Thorney Island experiments [14]) are strongly limited by flux-correction and thus quantities such as energy may not be precisely conserved. However, the energy loss in such simulations is reported by Hankin [8] to be some 10^3 times less than the work done against the ambient fluid in a resisted dense layer leading edge. It is thus the case that the total mechanical energy of a dense fluid layer is conserved to an acceptable degree of accuracy.

Note that a classical hydraulic jump is sometimes considered to be a discontinuous solution to the shallow water equations; this is sometimes called a 'weak solution'. Hydraulic jumps are considered more fully below.

6. The leading edge

As discussed in part 1 of this paper, the leading edge is modelled in such a way as to represent the hydrostatic force pushing the current forward and the drag offered by the ambient fluid. Although this method ignores the structure of the leading edge, it will be simulated in such a way as to control the following flow in the same way as a real current.

6.1. The leading edge in equilibrium with the following flow

The approximation of a constant front Froude number implies that the hydrostatic (forward) force is balanced by a momentum deficiency in the following flow of ambient fluid, following Benjamin [15]. It is important to show that the momentum interaction between dense layer and ambient fluid is simulated correctly as the method used is novel.

Fig. 1 shows a schematic view of a resisted dense layer moving from left to right. Dense fluid is forced in at the left hand side in such a way as to maintain a densimetric Froude number of unity at the point of entry. This should result in a current of uniform depth moving in solid body motion away from the source of fluid; at the front the hydrostatic force pushing the current forward is matched by the drag afforded by the ambient fluid through which the dense layer is intruding.

Fig. 2 thus shows an accurate simulation, with the exception of a slight numerical wiggle at the leading edge which appears to be a characteristic of FCT at a severe discontinuity. In view of the smallness of this oscillation (it persists but does not grow) and the fact that detailed simulation of the leading edge is not an objective, this behaviour is acceptable: the model is accurately simulating the leading edge as discussed above.

6.2. The leading control edge controlling the following flow

If there is a mismatch between the inflow conditions and the front condition, then the leading edge will exert an influence on the rest of the current; the leading edge is said to

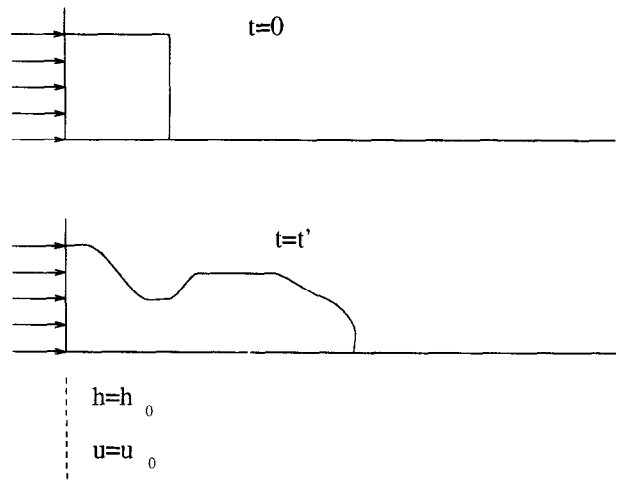

Fig. 1. Non-entraining one-dimensional gravity current: schematic view.

'control' the following flow. It is necessary for such behaviour to be reproducible as the influence of the leading edge may be considerable.

That the front can control the following flow is seen in Fig. 3 in which the leading edge condition is incompatible with the source on the left hand side. This has been done by changing the speed of the ambient fluid: the dense layer is now advancing into a headwind moving at half the speed of the inflow. As the front densimetric Froude number is defined relative to the ambient fluid and not the ground, the headwind is

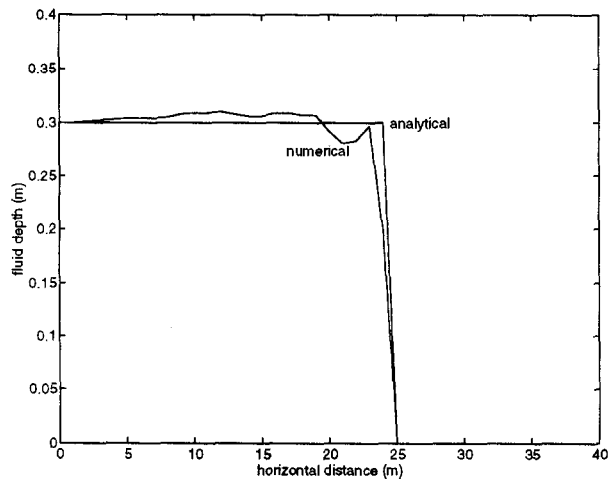

Fig. 2. Non-entraining one-dimensional gravity current: analytical and numerical predictions for stationary ambient fluid.

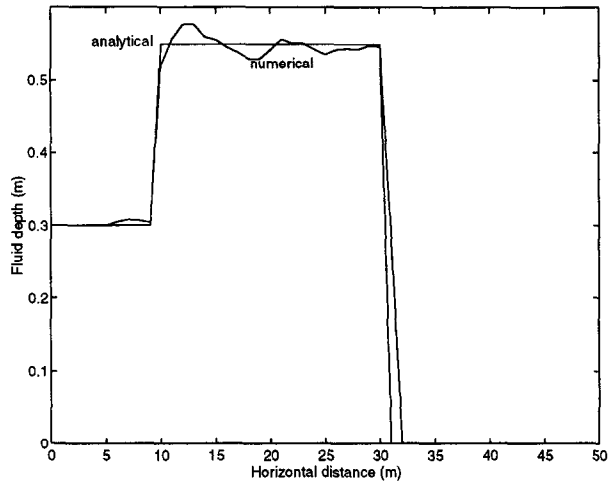

Fig. 3. Non-entraining one-dimensional gravity current in headwind: analytical and numerical predictions.

expected to force the current back; eventually a new equilibrium flow will be reached. There is an incompatibility between the inflow conditions and the leading edge.

The incompatibility causes a hydraulic jump which is close to the analytical prediction [3] also shown on the figure. The slight oscillations are due to transient waves that take a finite time to decay.

6.2.1. Hydraulic jumps and energy conservation

If only continuous solutions are considered, the shallow water equations conserve energy (Eq. (6)). However, the proof of Eq. (6) breaks down if discontinuous functions are admitted and it can be shown that energy is lost across a jump.

A hydraulic jump converts directed mechanical energy into random turbulent energy. In a hydraulic jump, therefore, some energy has to be dissipated and this occurs in nature by turbulent dissipation or waves. A term corresponding to the dissipation has been added to this in TWODEE and it is seen to perform satisfactorily. In the absence of this dissipative term, energy which would dissipate in a real hydraulic jump is carried away by waves that grow and eventually stop the simulation.

[3] The analytical prediction uses the hydraulic jump relation [16] and volume conservation on either side of the jump. If $R = y_2 / y_1$ is the ratio of downstream to upstream fluid depth, F and F_{IN} the densimetric Froude numbers at the front and inflow point, respectively, and $X = w / v_1$ the windspeed nondimensionalised with the inflow speed, then it can be shown that $R^4 - 2R^3 + 2R^2 - 2R[1 + F_{IN}(X - 1 + F/F_{IN})^2] + 1 = 0$. This system has one meaningful root with the specified parameters: $R \simeq 1.82$, which generated the analytical result.

6.3. Comparison of TWODEE results with the predictions of Grundy and Rottman [17] and Britter [18]

This section will compare the results of the present model with the analytical solutions given by Grundy and Rottman [17] and Britter [18]. These workers presented the radius of an axisymmetric dense current as a function of time, but here the area covered will be considered instead. This is because the radius of a dense current is not well defined in the present simulation but the area is exactly calculable.

The problem considered was that of the present study (that is, the shallow water equations together with a fixed, specified front Froude number β for the leading edge); entrainment was neglected.

6.3.1. Constant volume axisymmetric dense currents

In 1985, Grundy and Rottman [17] presented an analysis of planar and axisymmetric gravity currents. The axisymmetric results from that paper will be compared to those of the present code.

If a volume V of dense fluid of density ρ is released onto an infinite, smooth horizontal plane, then providing $\rho - \rho_a \ll \rho_a$, Grundy and Rottman [17] argued that the radius r_m of the dense layer at large times t will be asymptotic to

$$r_m = \left(\frac{16}{\pi}\right)^{1/4} \left\{\frac{\beta^2}{4-\beta^2}\right\}^{1/4} (Vg')^{1/4} t^{1/2}, \tag{7}$$

where g' is the reduced gravity $g(\rho - \rho_a)/\rho_a$ and β is the front Froude number. Here, t must be large compared to $x_0^2/(g'V)^{1/2}$ where x_0 is the initial radius of the dense fluid.

The test case chosen for comparison is the same as used by Hankin [8]; nondimensionalised results have been presented. The area of the dense layer as predicted by the present code and that predicted by Eq. (7) are shown in Fig. 4 to agree closely.

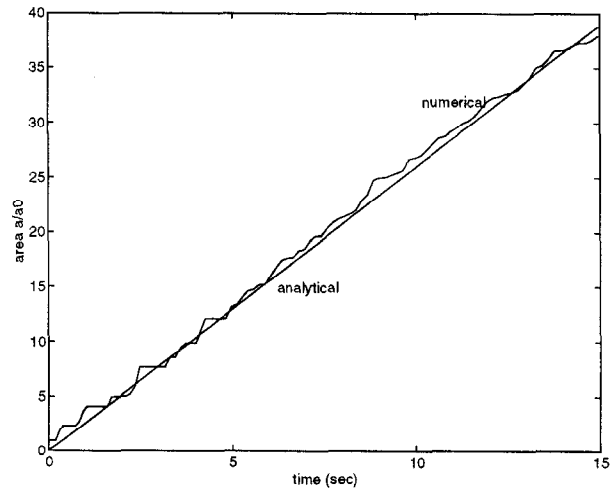

Fig. 4. Comparison of axisymmetric dense current areas: present work and Grundy and Rottman [17].

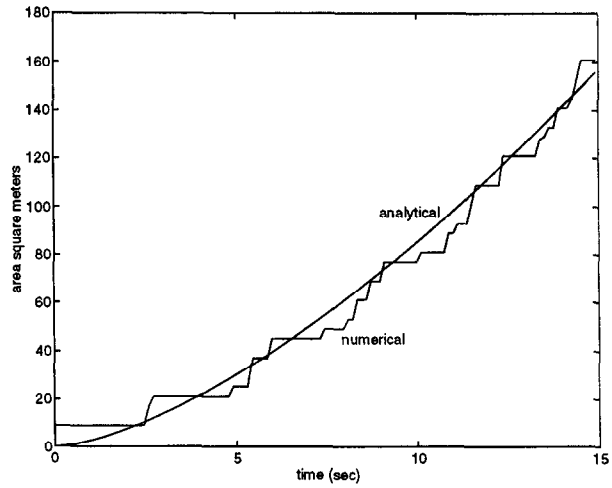

Fig. 5. Comparison of axisymmetric dense current areas: present work and Britter [18].

6.3.2. Constant flux axisymmetric dense currents

If the volume of the dense layer increases linearly with time, the system is said to be 'constant flux'. Britter [18] considered this problem and in an intuitively appealing argument gave the layer radius as:

$$r_m = \left(\frac{3}{4}\right)^{-3/4} \left(\frac{\alpha}{2\pi}\right)^{1/4} \beta^{1/2} (g'Q)^{1/4} t^{3/4} \tag{8}$$

where Q is the volume flow rate and α is an empirically determined dimensionless number. Britter then gave arguments to suggest that $\alpha = 1$.

Fig. 5 shows that the area of the dense layer as predicted by the current numerical scheme agrees closely with Eq. (8). The step-like appearance of the numerical curve is due to the computational discretization: the area increases discontinuously when a new fluid element has non-zero depth. The magnitude of the jumps is proportional to the gridsize used.

7. Summary

The numerical scheme under development has been checked in a number of ways in this paper. The advection scheme, being required to eliminate numerical overshoot completely, performs adequately. A number of analytical results have been simulated accurately.

There is thus confidence that the computational model solves the discretized shallow water equations accurately.

References

[1] S.T. Zalesak, Fully multidimensional flux-corrected transport algorithms for fluids, Journal of Computational Physics 31 (1979) 335–362.
[2] D.P. Chock, A comparison of numerical methods for solving the advection equation, part 2, Atmospheric Environment 19 (4) (1985) 571–586.
[3] P. Woodward, P. Colella, The numerical simulation of two-dimensional fluid flow with strong shocks (review article), Journal of Computational Physics 54 (1984) 115–173.
[4] J.P. Boris, D.L. Book, Flux-corrected transport: 1. SHASTA, a fluid transport algorithm that works, Journal of Computational Physics 11 (1973) 38–69.
[5] J.P. Boris, D.L. Book, Flux-corrected transport: 3. Minimal-error FCT algorithms, Journal of Computational Physics 20 (1976) 297.
[6] J.P. Boris, D.L. Book, K. Hain, Flux-corrected transport: 2. Generalisations of the method, Journal of Computational Physics 18 (1975) 248–283.
[7] G.A. Sod, Numerical Methods in Fluid Dynamics: Initial- and Initial Boundary-Value Problems, Cambridge Univ. Press, 1985.
[8] R.K.S. Hankin, Heavy gas dispersion over complex terrain, PhD thesis, Cambridge University, 1997.
[9] D.M. Webber, On the stability of spreading pool solutions of the shallow-water equations, Technical Report SRD/HSE R479, AEA Technology, Wigshaw Lane, Culcheth, Cheshire, WA3 4NE, January 1992.
[10] P.J. Roache, Computational Fluid Dynamics, Hermosa, 1982.
[11] H.P. Miller, A comparison of high resolution schemes for the two dimensional linear advection equation, Computers and Fluids 14 (4) (1986) 411–422.
[12] D.P. Chock, A.M. Dunker, A comparison of numerical methods for solving the advection equation, Atmospheric Environment 17 (1) (1983) 11–24.
[13] D.W. Pepper, C.D. Kern, P.E. Long, Modelling the dispersion of atmospheric pollution using cubic splines and chapeau functions, Atmospheric Environment 13 (1979) 223–259.
[14] J. McQuaid, B. Roebuck, The dispersion of heavier-than-air gas from a fenced enclosure. Final report to the U.S. Coast Guard on contract with the Health and Safety Executive, Technical Report RPG 1185, Safety Engineering Laboratory, Research and Laboratory Services Division, Broad Lane, Sheffield S3 7HQ, UK, 1985.
[15] T.B. Benjamin, Gravity currents and related phenomena, Journal of Fluid Mechanics 31 (2) (1968) 209–248.
[16] J.E. Simpson, Gravity Currents in the Environment and the Laboratory, Ellis Horwood, 1987.
[17] R.E. Grundy, J.W. Rottman, The approach to self-similarity of the solutions of the shallow-water equations representing gravity-current releases, Journal of Fluid Mechanics 156 (1985) 39–53.
[18] R.E. Britter, The spread of a negatively buoyant plume in a calm environment, Atmospheric Environment 13 (1979) 1241–1247.